Molecular Cancer Research

Oncogenes and Tumor Suppressors

Internalization by Multiple Endocytic Pathways and Lysosomal Processing Impact Maspin-Based Therapeutics

Thomas M. Bodenstine[1], Richard E. B. Seftor[1], Elisabeth A. Seftor[1], Zhila Khalkhali-Ellis[1], Nicole A. Samii[1], J. Cesar Monarrez[1], Grace S. Chandler[1], Philip A. Pemberton[2], and Mary J. C. Hendrix[1]

Abstract

Patients with metastatic disease face high rates of mortality with a paucity of therapeutic options. Protein-based therapeutics provide advantages over traditional chemotherapy through increased specificity, decreased immune impairment, and more direct means of delivery. However, development is often hindered because of insufficient knowledge about protein processing by cells when exogenously applied. This study focuses on recombinant Maspin (rMaspin), a serine protease inhibitor (SERPINB5), which alters invasive properties when directly applied to cancer cells. Previous evidence suggests differences in the effects of rMaspin treatment when compared with endogenous reexpression, with little explanation for these discrepancies. A leading hypothesis is that exogenously applied rMaspin is subject to different regulatory and/or processing mechanisms in cancer cells when compared with endogenous expression. Therefore, a more detailed understanding of the mechanisms of internalization and subcellular trafficking of rMaspin is needed to guide future translational development. We describe the molecular trafficking of rMaspin in cytoplasmic vesicles of the endosomal/lysosomal pathway and characterize its uptake by multiple endocytic mechanisms. Time-lapse laser scanning confocal microscopy shows the uptake, in real time, of dye-labeled rMaspin in cancer cells. This study indicates that cellular processing of rMaspin plays a key role by affecting its biologic activity and highlights the need for new approaches aimed at increasing the availability of rMaspin when used to treat cancer.

Implications: Novel characterization of internalization and subcellular trafficking of rMaspin provides new insights for future therapeutic development. *Mol Cancer Res; 12(10); 1480–91. ©2014 AACR.*

Introduction

Breast cancer remains the second leading cause of cancer-related mortality in women and represents the highest incidence of female cancer with approximately 1 in 8 women being diagnosed with breast cancer in their lifetime (1). Although more advanced screening methods combined with breast cancer awareness campaigns have increased early detection and improved overall life expectancy, the 5-year survival rate for patients with breast cancer with metastatic disease remains poor at 24%, compared with a 99% survival rate when the tumors remain localized. These statistics highlight the importance of developing therapies that act to reduce a patient's tumor burden and inhibit its metastatic spread.

Protein-based therapeutics provide many advantages over conventional cancer therapies (e.g., chemotherapy and radiation) and include higher target specificity, reduced immunologic impairment, and eliminate the need for transgene expression of tumor suppressor genes (2). Recombinant protein technology has been key to implementation of these therapies by providing efficient means of production and allowing for genetic manipulation of protein sequence(s) for increased specificity. However, the development of proteins as anticancer treatments remains challenging (3). Significant hurdles exist related to the efficient delivery of recombinant proteins, their uptake, proper function, and clearance by target cancer cells, which require detailed scrutiny.

Maspin is a unique and noninhibitory member of the Serpin superfamily originally described as a tumor suppressor in breast cancer (4). Previous reports in cancer cells have demonstrated that Maspin inhibits cellular migration and invasion, reduces angiogenesis, and increases cancer cell sensitivity to apoptosis signals, all of which act to reduce the aggressive cancer cell phenotype (5–7). Maspin's effects have been attributed to interactions with proteins at different

[1]Stanley Manne Children's Research Institute, Cancer Biology and Epigenomics Program, Northwestern University Feinberg School of Medicine, Robert H. Lurie Comprehensive Cancer Center, Chicago, Illinois. [2]SerPlus Technology LLC, Belmont, California.

Note: Supplementary data for this article are available at Molecular Cancer Research Online (http://mcr.aacrjournals.org/).

Corresponding Author: Mary J. C. Hendrix, Stanley Manne Children's Research Institute, Children's Research Fund Professor William G. Swartchild, Jr. Distinguished Research Professor, Robert H. Lurie Comprehensive Cancer Center, Northwestern University Feinberg School of Medicine, Chicago, IL. Phone: 773-755-6528; Fax: 773-755-6534; E-mail: m-hendrix@northwestern.edu

doi: 10.1158/1541-7786.MCR-14-0067

cellular locations as well as within the extracellular environment (6, 8–10). These observations are further supported by clinical data demonstrating that the prognostic implications of Maspin are governed by its subcellular localization (9, 11).

Recombinant Maspin (rMaspin) added to certain cancer cells recapitulates some of the inhibitory effects on tumor cell aggressiveness that have been reported when Maspin is endogenously expressed with respect to suppression of invasion and migration (7, 12, 13). Other effects related to cytosolic functions of Maspin have not been reproduced (14, 15), with no clear explanation for the observed discrepancies. In addition, the mechanisms of rMaspin uptake by cancer cells and processing after entry remain unexplored—critical information for utilizing rMaspin in therapeutic approaches. This study was undertaken to examine the route(s) of entry of rMaspin into cancer cells, its subcellular localization, and ultimate fate to help guide future translational studies. We demonstrate that rMaspin is internalized *via* multiple mechanisms of endocytosis and transported to the lysosome, a process that limits its cytosolic interactions and nuclear localization. These observations suggest that therapeutic approaches that induce the escape of rMaspin from endosomes or lead to alternative internalization of exogenously applied rMaspin may contribute to the efficacy of rMaspin as a breast cancer therapeutic.

Materials and Methods

Recombinant Maspin and Alexa Fluor 594 labeling

Highly purified rMaspin (SerPlus Technology, LLC) was expressed and purified from yeast *S. cerevisiae*, and stored in 10 mmol/L sodium phosphate, 130 mmol/L sodium chloride, pH 7.5. Aliquots were frozen at $-80°C$ and thawed on ice at time of experiment. Purified Maspin was >95% pure by SDS-PAGE, >95% monomer content by size exclusion HPLC, >98% pure by reverse-phase HPLC, and contained <0.05 endotoxin units (EU) per mg of protein. For experiments using fluorescently labeled rMaspin, Alexa Fluor 594 carboxylic acid, succinimidyl ester (Life Technologies) was conjugated to rMaspin according to the manufacturer's protocol. Briefly, purified rMaspin was reacted with Alexa Fluor 594 under basic conditions in a sodium biocarbonate buffer and column purified using a Bio-Rad BioGel P-30 fine size exclusion purification resin to remove free dye. Use of a NanoDrop 1000 Spectrophotometer to analyze dye to protein ratio following label demonstrated a ratio of 1.39 and correlated to a minor increase in molecular weight observed by immunoblot analysis (shown in Supplementary Fig. S2).

Cell culture

The MDA-MB-231 invasive breast cancer cell line (American Type Culture Collection; ATCC) was grown in DMEM/F12 (Life Technologies) supplemented with 5% FBS, minimal essential amino acids, and gentamycin. Hs578T and BT549 (ATCC) breast cancer cell lines were grown in RPMI (Life Technologies) supplemented with 10% FBS and gentamycin. The MCF10A (ATCC) cell line was derived from a spontaneous immortalization of epithelial cells in a patient with fibrocystic disease and was cultured in DMEM/F12 (Life Technologies) supplemented with 5% horse serum, 20 ng/mL EGF, 0.5 mg/mL hydrocortisone, 100 ng/mL cholera toxin, and 10 μg/mL insulin. Cell lines were authenticated by short tandem repeat genotyping by PCR amplification at the Molecular Diagnostic/HLA Typing Core at Ann and Robert H. Lurie Children's Hospital of Chicago (2009–2010). Cell lines were used for less than 6 months after thaw. All cultures were routinely screened for *Mycoplasma* (Roche) and found to be free of contamination.

Confocal fluorescence microscopy

Cells were grown on glass coverslips with indicated treatments and fixed in ice cold methanol, blocked in 2% BSA, and incubated with primary antibodies. Coverslips were mounted on glass slides using VectaShield with DAPI (Vector Laboratories). Confocal images were obtained on a Zeiss 510 META Confocal Laser Scanning Microscope. For live cell imaging, cells were grown in MatTek glass bottom micro dishes, and time-lapse fluorescence confocal microscopy was recorded on a Zeiss 700 Confocal Laser Scanning Microscope equipped with a LSM 700 XL S1 incubation system. Time-lapse confocal fluorescence and differential interference contrast (DIC) microscopy images were recorded at 60-second intervals over 16 hours. Immunofluorescence data were analyzed using Zeiss ZEN 2009 Windows-based software. The subcellular and vesicular localization patterns of rMaspin described in this study were confirmed by z-stack analysis and three-dimensional rendering.

Cell lysis

Whole-cell lysates were prepared in 25 mmol/L Tris, pH 7.4, 0.5 mmol/L EDTA, 5% glycerol, 1% SDS, and 1× Complete Mini protease inhibitors (Roche) with passage through a 21-gauge needle 12× on ice. For nuclear/cytoplasmic separation, cells were lysed in 10 mmol/L HEPES buffer, pH 7.9, 10 mmol/L NaCl, 1 mmol/L dithiothreitol, 10% glycerol, 15 mmol/L $MgCl_2$, 0.2 mmol/L EDTA, and 0.1% Nonidet P-40. Lysates were freeze/thawed 3× and centrifuged at 4,500 × *g* for 10 minutes. The supernatant containing cytosolic fraction was removed, and the pellet washed 2× with lysis buffer, then resuspended in lysis buffer + 500 mmol/L NaCl on ice for 30 minutes with periodic vortexing. The suspension was centrifuged at 25,000 × *g* for 20 minutes to obtain the nuclear fraction.

Reagents and antibodies

Chemical inhibitors chloroquine, dansylcadaverine, and nystatin were purchased from Sigma. Recombinant receptor-associated protein was kindly provided by Dr. Andrew Mazar, Northwestern University (Evanston, IL). For inhibitor experiments, cells were serum starved for 60 minutes before treatments. Fluorescein isothiocyanate dextran 70,000 molecular weight conjugate (FITC-Dextran) was purchased from Sigma. Endo-porter was purchased from Gene Tools, LLC. Detailed information about the antibodies used in this study is listed in Supplementary Table S1.

Invasion assay

Control or siRNA transfected MDA-MB-231 cells were pretreated as indicated for 24 hours followed by seeding of cells (5×10^4) into upper wells of the MICS (membrane invasion culture system; 16) chamber onto intervening collagen IV/laminin gelatin-coated (Sigma) polycarbonate membranes containing 10-μm pores (Whatman) in RPMI-1640 with 1× MITO+ (BD Biosciences). Cells were grown with indicated treatments for 24 hours. Invading cells were collected, stained, and counted as previously described (17). Percent invasion was corrected for proliferation and calculated as total number of invading cells/total number of cells seeded × 100 and normalized to controls. Statistical significance was determined by the Student *t* test. Data are expressed as mean ± SD. Statistical significance was set at a value of $P < 0.05$ (*).

Immunoblot analyses

Protein concentrations for lysates were determined by BCA assay (Thermo Scientific) and diluted in Laemmli Sample Buffer (Bio-Rad) supplemented with β-mercaptoethanol and boiled for 10 minutes at 95°C. 12% SDS-PAGE with 4% stacking gels were used to resolve lysates, with 10 μg of protein loaded per lane. Proteins were transferred to polyvinylidene difluoride (PVDF) membranes (Bio-Rad) and identified using the appropriate primary and secondary antibodies + HRP with chemiluminescence detection. ImageJ (NIH) software was used for densitometry analysis.

Plasmids and transfection methods

Maspin was cloned into the pEGFP-C2 plasmid to fuse Maspin to the enhanced GFP (EGFP) with expression driven by the human cytomegalovirus immediate early promoter. The Maspin gene was followed by an SV40 early mRNA polyadenylation signal. The plasmid was grown in One Shot TOP10 Chemically Competent *Escherichia coli* (Life Technologies) using kanamycin selection and subsequently isolated using the Plasmid Maxi-Prep protocol (Qiagen). Lipofectamine LTX and PLUS Reagent (Life Technologies) were used to transfect cells as per the manufacturer's protocol.

siRNA

Silencer Select validated siRNA targeting human clathrin heavy chain (Entrez Gene ID: 1213) and Silencer Select Negative Control No.1 (non-silencing control; NSC) were purchased from Life Technologies. Following siRNA optimization experiments as per the manufacturer's protocol, siPORT *NeoFx* reagent was used to transfect 25 nmol/L siRNA into MDA-MB-231 for 48 hours. Transfection media were then removed and cells grown in complete media for an additional 48 hours. Knockdown of clathrin heavy chain protein was confirmed via immunoblot and immunofluorescence analysis.

Results

rMaspin is limited to cytoplasmic vesicles following internalization and atypical of endogenously expressed protein

Although previous reports have evaluated the biologic effects of exogenously applied rMaspin on cancer cells (7, 12, 13), the internalization mechanisms, subcellular processing, and/or clearance of rMaspin were not characterized. To further elucidate the processes involved, we began by analyzing the localization of endogenously expressed Maspin protein compared with that of rMaspin following internalization by cancer cells. rMaspin was labeled with Alexa Fluor 594 dye (rMaspin^{594}) for use as a detection tool in our study. rMaspin^{594} was added to the growth media of the endogenous Maspin expressing mammary epithelial cell line MCF10A. Endogenous Maspin fluorescence was detected with an Alexa Fluor 488 secondary antibody and localization patterns for each protein were analyzed by confocal microscopy. The images reveal that endogenously expressed Maspin was localized diffusely throughout the cell while rMaspin^{594} exhibited a vesicular appearance confined to the cytoplasm (Fig. 1A). To examine whether these localization patterns differed among breast cancer cells, we transiently transfected Maspin-null MDA-MB-231 and Hs578T breast cancer cell lines with an expression plasmid containing a Maspin EGFP fusion protein (Maspin^{EGFP}), and these cells were subsequently treated with rMaspin^{594}. Similar to endogenously expressed Maspin, transgene expression led to Maspin^{EGFP} protein localization throughout the cytosol while rMaspin^{594} maintained a vesicular appearance (Fig. 1B). Because transfection efficiency was <100%, we were able to evaluate rMaspin^{594} uptake in nontransfected cells which exhibited the same localization patterns, indicating that rMaspin is internalized independent of mechanisms regulated by endogenously expressed Maspin. Detection of unlabeled rMaspin with an Alexa Fluor 594–labeled secondary antibody produced similar staining patterns when compared with rMaspin^{594} (Supplementary Fig. S1), thereby validating the fluorescence patterns observed in the microscopy experiments. Collectively, these results demonstrate important differences in the fate of endogenously expressed compared with exogenously applied Maspin protein.

The vesicular appearance of rMaspin^{594} following cellular internalization in our initial experiments suggested potential uptake by endocytosis, an energy, and temperature-dependent process responsible for internalization of components from the extracellular environment. To evaluate whether rMaspin^{594} uptake occurred through active transport mechanisms indicative of endocytosis, MDA-MB-231, Hs578T, and BT549 cells were treated with rMaspin^{594} and grown at 37°C, or 4°C to limit cellular internalization pathways to passive and/or facilitated diffusion. Internalization of rMaspin^{594} in each cell line was dramatically reduced at 4°C when compared with growth at 37°C (Fig. 1C). Although some Maspin^{594} seemed to enter the cell at low temperature, these results suggested

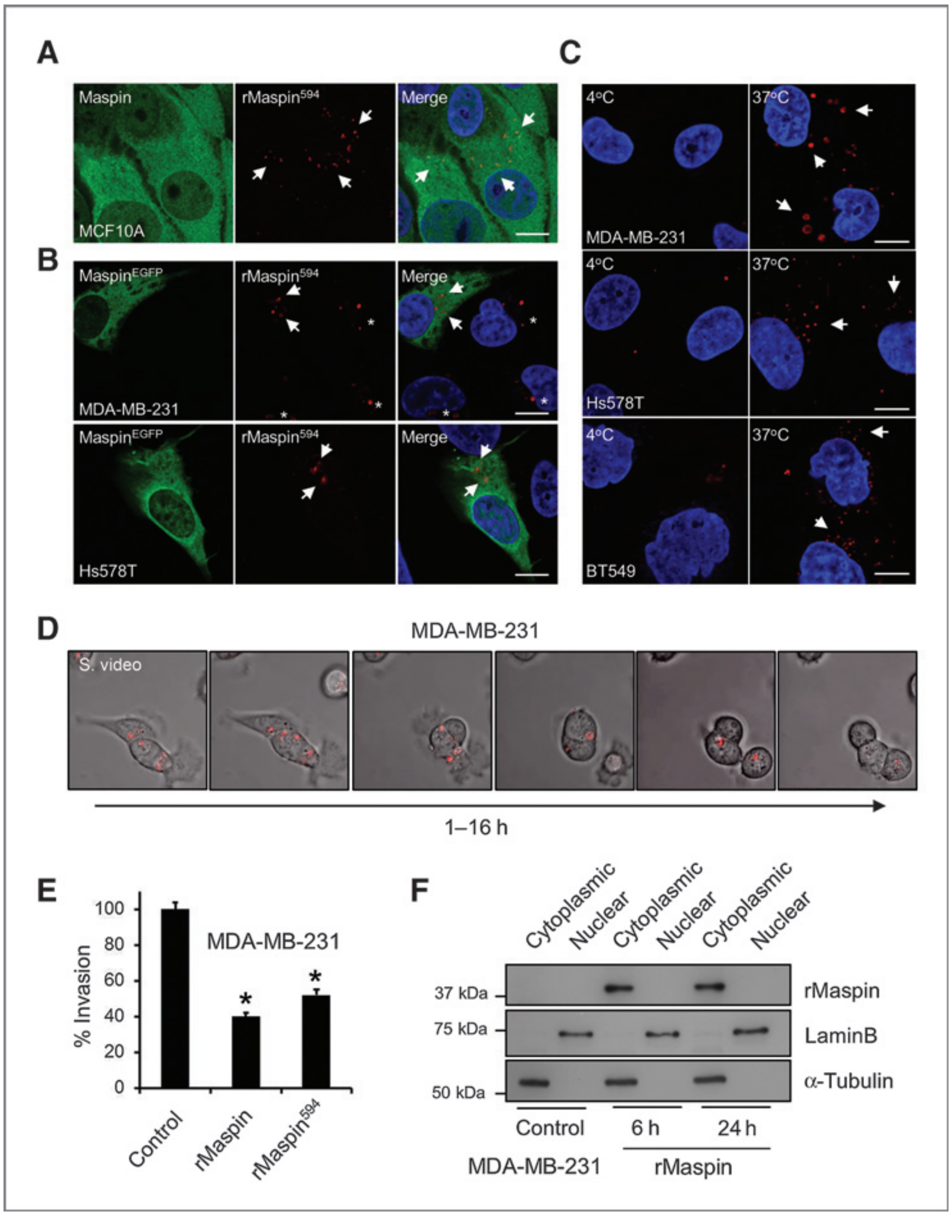

Figure 1. rMaspin subcellular localization is distinct from genetic expression. A, endogenous Maspin expressing MCF10A cells were treated with Alexa Fluor–labeled rMaspin^{594} (10 μg/mL for 60 minutes). Fluorescence patterns of rMaspin^{594} (red) were compared with endogenous Maspin detected with an Alexa Fluor 488 secondary antibody (green) by confocal microscopy. B, MDA-MB-231 and Hs578T cells were treated with rMaspin^{594} (red) as in A, following transfection with a Maspin^{EGFP} transgene (green). Asterisks denote rMaspin^{594} fluorescence in cells that did not express plasmid. C, MDA-MB-231, Hs578T, and BT549 cells were treated with rMaspin^{594} (10 μg/mL for 60 minutes) and grown at 4°C or 37°C to allow for passive/facilitated diffusion and temperature dependent-active transport mechanisms, respectively. A–C, nuclei counterstained with DAPI (blue); scale bar represents 10 μm; arrows highlight rMaspin^{594} vesicles. D, to observe vesicular localization of rMaspin in real-time, MDA-MB-231 were grown in media containing rMaspin^{594} (30 μg/mL) for 16 hours in an environmental chamber. rMaspin^{594} fluorescence (red) and DIC images were collected by confocal microscopy at 60-second intervals (Supplementary Video). E, MDA-MB-231 cells were pretreated with or without rMaspin or rMaspin^{594} (30 μg/mL for 24 hours) and grown in a three-dimensional membrane invasion culture system in the presence or absence of rMaspin or rMaspin^{594} (30 μg/mL for 24 hours). Percent invasive cells were quantified and normalized to control conditions (*, $P < 0.05$, $n = 3$). F, MDA-MB-231 cells were treated with rMaspin (30 μg/mL) for 6 and 24 hours. Nuclear and cytoplasmic cell fractions were collected and probed with Maspin antibody. α-tubulin (cytoplasmic) and Lamin B (nuclear) antibodies were used for loading controls and designate fraction purity. (Hs578T and BT549 shown in Supplementary Fig. S3).

that the majority of rMaspin^{594} internalization occurred through active mechanisms.

We next sought to visualize this trafficking process in live cells. MDA-MB-231 cells were continuously treated with rMaspin^{594} and observed using time-lapse laser scanning confocal microscopy in an environmental chamber. In confirmation of our endocytosis experiments, rMaspin^{594} fluorescence was predominately observed within cytoplasmic vesicles and at the cell membrane (Fig. 1D; Supplementary Video). The time-lapse video analysis allowed for observation of the dynamic trafficking of rMaspin^{594} within these vesicles as they were subjected to sorting signals. Morphologic changes, including retraction of cellular pseudopodia, were noted approximately 4 hours following treatment and correlated with previous reports demonstrating reduced invasive qualities of rMaspin-treated cancer cells. To validate the results observed in our time-lapse analysis, we demonstrated that dye labeling of rMaspin^{594} led to a slight shift in molecular weight that was maintained following cellular internalization (Supplementary Fig. S2A and S2B). This indicated that the dye remained stably attached with no formation of cleavage products, thus decreasing the likelihood of unconjugated dye fluorescence. When compared with unconjugated rMaspin, rMaspin^{594} retained its ability to significantly inhibit cellular invasion of MDA-MB-231 cells through three-dimensional matrix, validating the uptake of a stable, biologically active rMaspin^{594} with inhibitory effects on invasion (Fig. 1E).

Recent work has indicated the importance of the nuclear functions of Maspin on tumorigenicity (9, 11). Thus, we combined our video microscopy results with immunoblot analysis of cell lysates from cytoplasmic and nuclear fractions of treated cells, which did not indicate nuclear association of rMaspin (Fig. 1F and Supplementary Fig. S3). Taken together, our characterization of rMaspin^{594} demonstrates

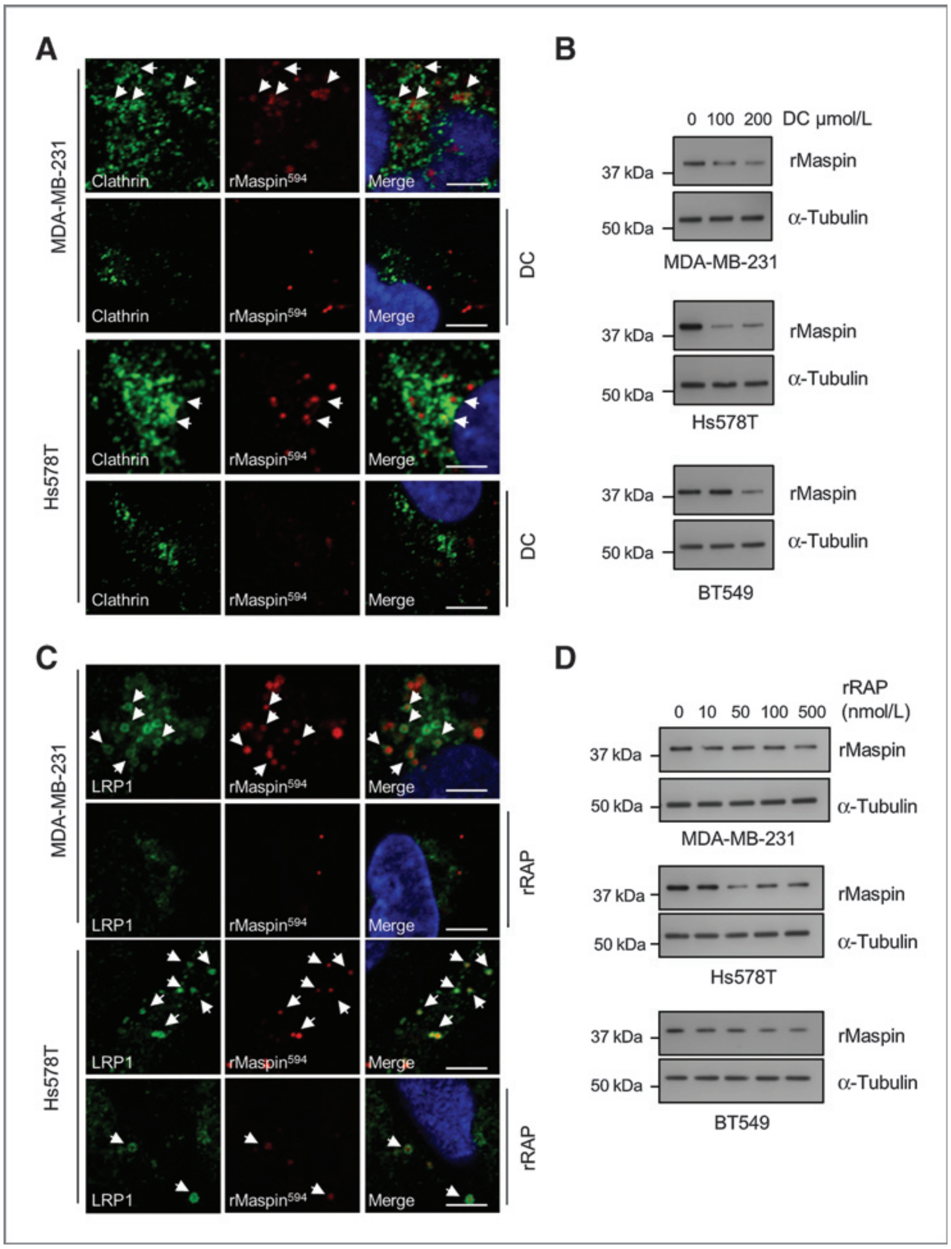

Figure 2. rMaspin is internalized via receptor-mediated endocytosis mechanisms. A, MDA-MB-231 and Hs578T cells were treated with rMaspin^{594} (10 μg/mL for 60 minutes) in the presence or absence of DC (200 μmol/L; 30-minute pretreatment). rMaspin^{594} (red) localization was compared with clathrin (green) to mark endocytic vesicles and analyzed by confocal microscopy. B, representative lysates from cells treated with rMaspin as in A, with indicated concentrations of DC (100–200 μmol/L, 30-minute pretreatment) and immunoblotted with Maspin and α-tubulin antibodies. C and D, cells were treated with rMaspin as in A and B with recombinant RAP (rRAP) treatments at indicated concentrations (10–500 nmol/L, 30-minute pretreatment). C, rMaspin^{594} fluorescence (red) was compared with LRP1 (green) in the presence or absence of rRAP (500 nmol/L). D, representative immunoblot analyses of lysates from rMaspin and rRAP-treated cells probed with Maspin and α-tubulin antibodies. A and C, nuclei were counterstained with DAPI; scale bar, 5 μm; arrows highlight rMaspin^{594} within clathrin (A) and LRP1 (C) vesicles.

its inclusion into cytoplasmic vesicles while maintaining the inhibitory effect on cancer cell invasion. Therefore, we set out to examine the mechanisms of the internalization processes and their implications on rMaspin function and translational development.

rMaspin associates with multiple early markers of endocytosis

Our results about the temperature dependency of rMaspin^{594} uptake prompted analysis of internalization pathways and the nature of the vesicles that contain rMaspin^{594}. Receptor-mediated endocytosis (RME) is a common pathway involved in the internalization of receptors, ligands, and protein complexes (18). Given the reported binding interactions of Maspin with membrane proteins internalized by this mechanism (19, 20), we began our analysis by examining this pathway. We evaluated rMaspin^{594} uptake with clathrin, a well-characterized protein that forms structural complexes around budding endocytic vesicles associated with RME (21). Following treatment of breast cancer cells, we found rMaspin^{594} within clathrin-bound vesicles as assessed by confocal fluorescence microscopy and when cells were pretreated with dansylcadaverine (DC), an inhibitor of clathrin-mediated endocytosis, the presence of rMaspin^{594} in these vesicles was greatly reduced (Fig. 2A). Pretreatment of cells with DC led to decreased rMaspin in whole-cell lysates (Fig. 2B), in agreement with immunofluorescence data indicating reduced internalization through this pathway. As confirmatory evidence for the role of RME on rMaspin endocytosis, we examined uptake with a second protein, the low-density lipoprotein receptor-related protein 1 (LRP1). LRP1 is a membrane protein that binds to receptors and ligand complexes, facilitating RME (22). We observed rMaspin^{594} within LRP1 vesicles in the cytoplasm of breast cancer cells following internalization (Fig. 2C). To modulate LRP1 availability at the plasma membrane, we treated cells with recombinant receptor associated protein (rRAP), an intracellular chaperone of LRP1 that when added exogenously induces endocytosis and recycling of LRP1. This approach

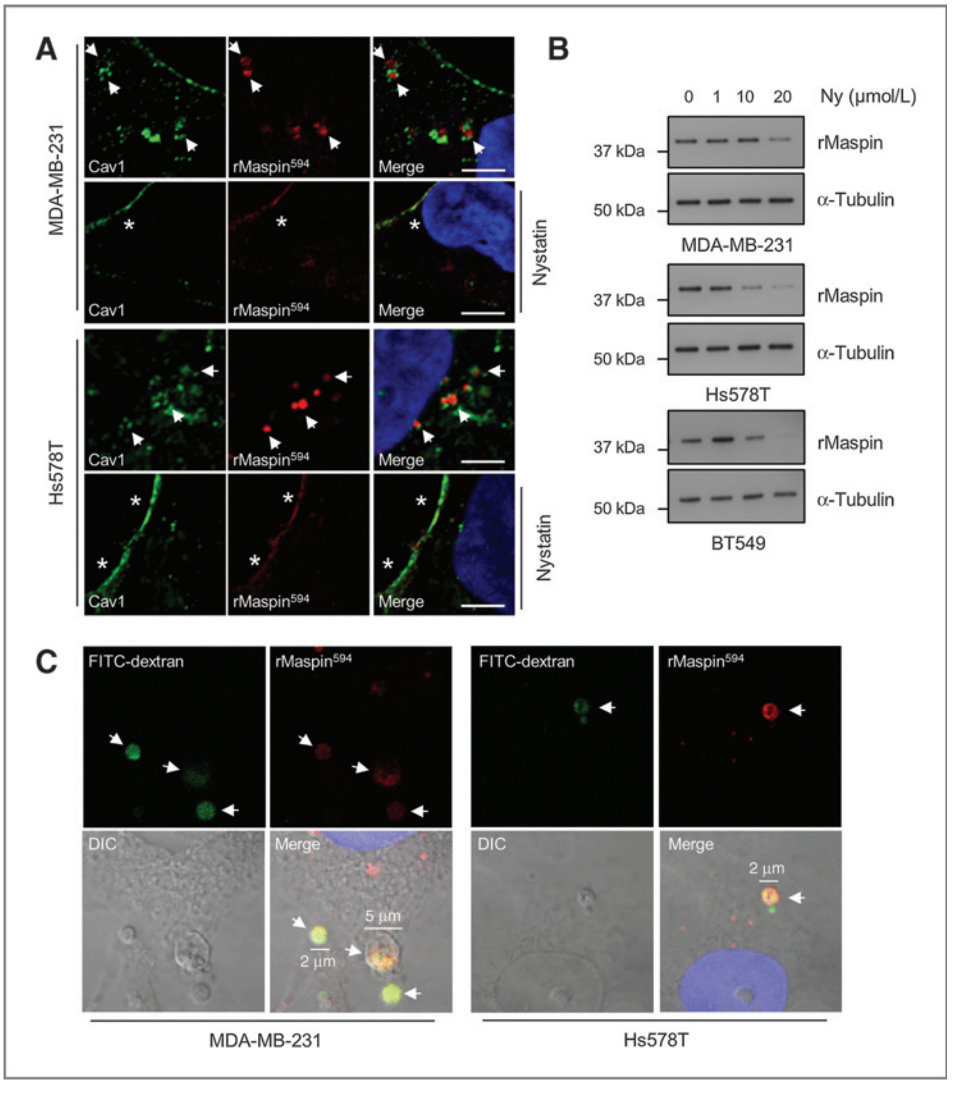

Figure 3. rMaspin associates with multiple early markers of endocytosis. A, MDA-MB-231 and Hs578T cells were treated with rMaspin^{594} (10 μg/mL for 60 minutes) in the presence or absence of nystatin (Ny, 20 μmol/L; 30-minute pretreatment). Fluorescence localization of rMaspin^{594} (red) was compared with the lipid raft marker caveolin 1 (Cav1; green) by confocal microscopy. Arrows highlight rMaspin^{594} within Cav1 vesicles; asterisks denote accumulation of rMaspin^{594} and Cav1 at the plasma membrane; scale bar, 5 μm. B, MDA-MB-231, Hs578T, and BT549 cells were treated with rMaspin as in A, in the presence or absence of Ny (1–20 μmol/L; 30-minute pretreatment). Lysates were immunoblotted with Maspin and α-tubulin antibodies. C, MDA-MB-231 and Hs578T were cotreated with FITC-dextran (2.5 μg/mL) and rMaspin^{594} (10 μg/mL) for 60 minutes and analyzed by confocal fluorescence microscopy. Arrows highlight areas of FITC-dextran and rMaspin^{594} colocalization. A and C, nuclei were counterstained with DAPI.

decreases the availability of LRP1 at the plasma membrane. Consistent with internalization through RME-related pathways, pretreatment with increasing concentrations of rRAP led to a decrease in the association of rMaspin^{594} with LRP1 vesicles (Fig. 2C) and reduced rMaspin protein in cell lysates (Fig. 2D). Collectively, these experiments indicate that rMaspin internalization can be reduced by modulating clathrin and LRP1 dynamics, and provides evidence for the transport of rMaspin at the plasma membrane into the cell through RME pathways.

Interestingly, neither DC or rRAP treatment fully inhibited the vesicular uptake of rMaspin^{594}, suggesting the existence of additional internalization processes. This led us to investigate whether rMaspin^{594} could be internalized by other endocytic pathways. Endocytosis by lipid rafts occurs through vesicle formation from organized micro-domains in the plasma membrane enriched in cholesterol and glycosphingolipids (23). Caveolin 1 (Cav1) is a structural membrane protein involved in the internalization of caveolae lipid rafts, and used as a marker of this process. rMaspin^{594} associated with Cav1 vesicles in breast cancer cell lines and suggested the potential involvement of lipid rafts on the internalization of rMaspin^{594} (Fig. 3A). Lipid raft endocytosis can be reduced by the sequestering of cholesterol in the plasma membrane and decreasing fluidity of these micro-domains (24). When cells were pretreated with nystatin, a cholesterol sequestering agent, rMaspin^{594} accumulated at the plasma membrane, and Cav1 vesicles containing rMaspin^{594} in the cytoplasm decreased (Fig. 3A). In confirmation of these observations, pretreatment with nystatin resulted in decreased rMaspin protein levels in whole-cell lysates (Fig. 3B). It should be noted that cholesterol sequestration has secondary effects on other types of endocytosis pathways which may contribute to the accumulation of rMaspin^{594} observed at the cell membrane (21, 24). However, a primary effect on lipid rafts with nystatin treatment is expected and validated by the relocalization of Cav1.

We next examined whether rMaspin^{594} could be internalized by generalized uptake of fluid from the extracellular environment. Macropinocytosis represents a major mechanism for the internalization of extracellular fluid through the formation of large plasma membrane-bound vesicles subsequently internalized by the cell. Uptake of dextran is a commonly used marker for macropinocytosis and denoted macropinosomes in our study. Following serum starvation, cells were cotreated with FITC-dextran and rMaspin^{594} and analyzed by confocal microscopy. The fluorescence of both molecules was visualized within macropinosomes that formed near the plasma membrane borders (Fig. 3C). These vesicles exhibited sizes from approximately 0.5 to 10 μm, within the range of typical macropinosomes. Taken together, these observations indicate that rMaspin internalization in cancer cells can be mediated through numerous pathways, and increases the diversity of potential interactions with other proteins that may take place during these processes.

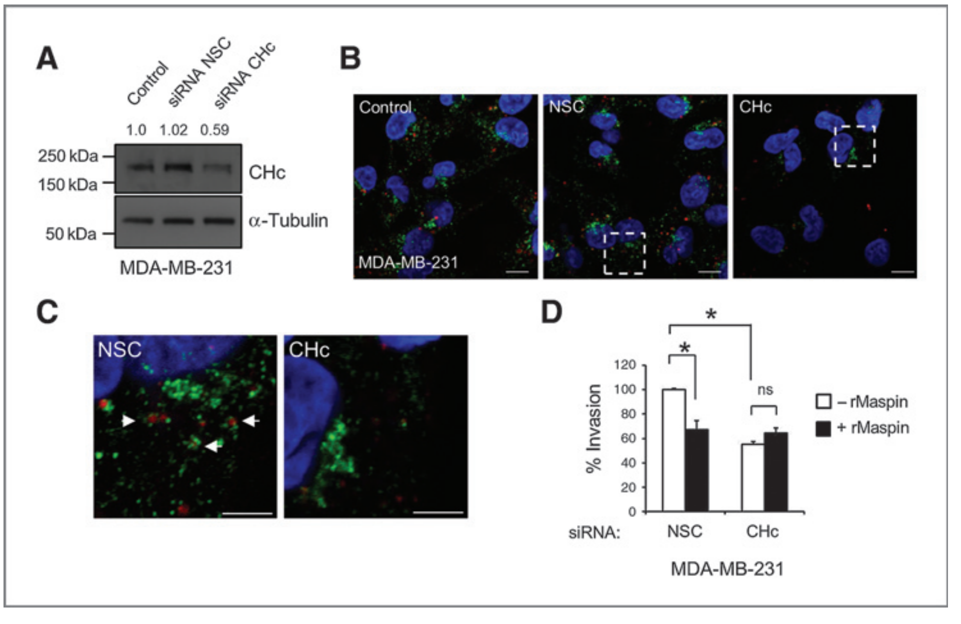

Figure 4. rMaspin treatment does not affect invasion of clathrin siRNA-treated cells. A, MDA-MB-231 cells were transfected with siRNA targeting CHc or NSC siRNA for 48 hours. At 48 hours after removal of transfection media CHc protein expression was analyzed by immunoblot analysis with clathrin and α-tubulin antibodies. Densitometric values were corrected for α-tubulin and normalized to control. B, confocal immunofluorescence of CHc (green) in MDA-MB-231 treated with rMaspin^{594} (red; 10 μg/mL for 60 minutes) following siRNA transfection of cells described in A. Scale bar, 10 μm. C, magnification of areas in B, showing MDA-MB-231 transfected with CHc or NSC siRNA treated with rMaspin^{594}. Arrows highlight clathrin bound rMaspin^{594} vesicles. Scale bar, 5 μm. B and C, nuclei were counterstained with DAPI (blue). D, MDA-MB-231 treated with CHc and NSC siRNA were pretreated with or without rMaspin (30 μg/mL for 24 hours) and grown in a three-dimensional membrane invasion culture system in the presence or absence of rMaspin (30 μg/mL for 24 hours). Percent invasive cells were quantified and normalized to siRNA negative control (*, $P < 0.05$, $n = 4$).

Effect of clathrin knockdown on invasion

Because clathrin regulates numerous membrane molecules involved in cellular motility, and Maspin binds to membrane components involved in cellular invasion, we questioned whether the induction of clathrin-mediated endocytosis by rMaspin was involved in the inhibition of invasion. To address this specifically, siRNA was used to knockdown clathrin heavy chain (CHc) in the invasive MDA-MB-231 cell line confirmed by immunoblot and immunofluorescence analysis (Fig. 4A and B). As expected, rMaspin^{594} internalization was reduced in clathrin vesicles when CHc was knocked down (Fig. 4C). These conditions allowed rMaspin to continue to interact with other components at the plasma membrane independent of regulation by clathrin. Similar to data in Fig. 1E, when NSC siRNA-transfected cells were treated with rMaspin, a significant decrease in invasion was observed (Fig. 4D). Interestingly however, disruption of clathrin-mediated endocytosis by knockdown of CHc exhibited a similar effect on invasion and addition of rMaspin to these cells did not produce a synergistic effect (Fig. 4D). These results suggest that regulation of molecules through clathrin endocytosis is necessary in part for the invasive qualities of MDA-MB-231 cells, and the inability of rMaspin to further reduce invasion in CHc knockdown cells suggests that rMaspin may act on molecules regulated by this pathway with respect to invasion.

rMaspin is trafficked as late endocytic cargo in breast cancer cells

Proteins internalized by endocytosis are subject to numerous sorting and subcellular routing mechanisms (21). Because we observed rMaspin^{594} in early vesicles of the endocytic pathway, we evaluated whether rMaspin^{594} was trafficked to later stages of endocytosis in MDA-MB-231, Hs578T, and BT549 cell lines. We examined the localization of rMaspin^{594} to Rab9, a small GTPase involved in endosomal trafficking and a marker of late endosomes. rMaspin^{594} was observed within Rab9-positive late endosomes, indicating that following internalization, rMaspin^{594} is exposed to the acidifying environment within the late endosomal lumen (Fig. 5A). As late endosomes continue to mature, cargo is subject to further sorting and recycling mechanisms, therefore, we determined whether the trafficking of rMaspin^{594} continues to the lysosome, a terminal vesicle of the endocytic process. Evaluation of Lamp1 (lysosome-associated membrane protein 1) fluorescence to mark the lysosomal membranes revealed the presence of rMaspin^{594} within these vesicles (Fig. 5B). Together, with our analysis of early endocytic markers, these data highlight the complete trafficking of rMaspin^{594} from the early to final stages of the endocytosis pathway. In line with this analysis, we observed that rMaspin was rapidly cleared from cells over time following treatment (Supplementary Fig. S4).

Decreased lysosomal activity increases rMaspin cellular accumulation

To confirm that rMaspin^{594} is cleared, in part, by the lysosomal pathway, we examined rMaspin-treated cells in the presence of the endosomal/lysosomal inhibitor chloroquine. Chloroquine is a lipophilic 4-aminoquinoline compound that incorporates into the endosomal pathway by association at the plasma membrane through its hydrophobic domain. Within the endosome, chloroquine exerts a buffering capacity that slows endosomal acidification and inhibits pH-dependent proteases after its arrival to the lysosome (25). Thus, treating cells with chloroquine has been used to reduce the degradation of proteins processed by this pathway. Breast cancer cells were pretreated with or without chloroquine before the addition of rMaspin. Immunoblot analysis of whole-cell lysates demonstrated that

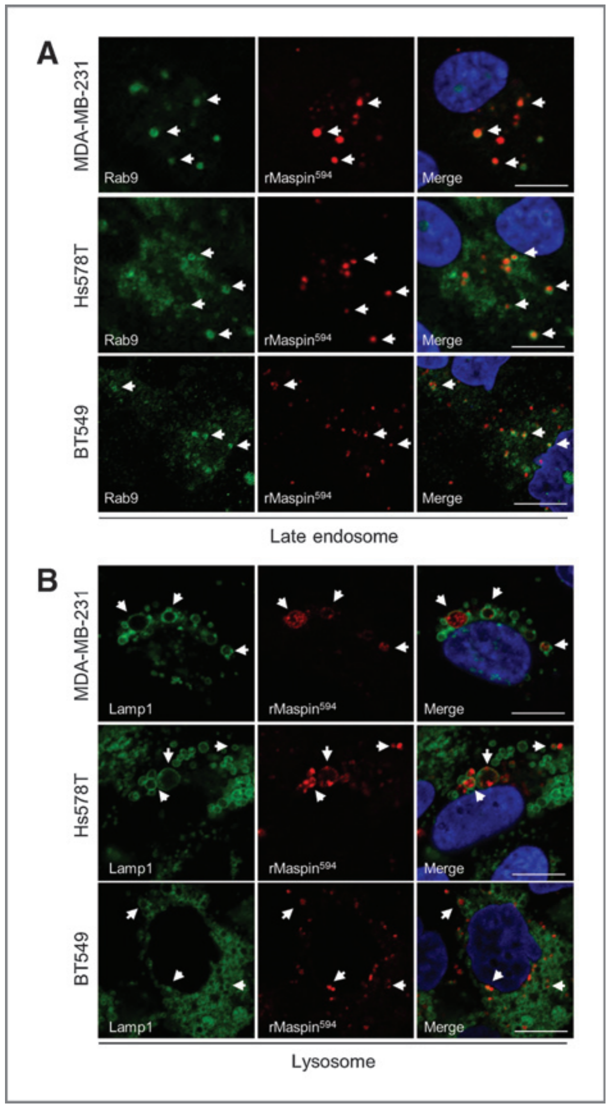

Figure 5. rMaspin is trafficked through the late endosomal/lysosomal pathway. MDA-MB-231, Hs578T, and BT549 cells were treated with rMaspin^{594} (10 μg/mL for 60–120 minutes). rMaspin^{594} fluorescence (red) was compared with localization with Rab9 late endosomes (green) at 60 minutes (A) and Lamp1 lysosomes (green) at 120 minutes (B) by confocal microscopy. Nuclei were counterstained with DAPI (blue); scale bar, 10 μm; arrows highlight rMaspin^{594} vesicles within late endosomes (A) and lysosomes (B).

rMaspin accumulated in the chloroquine treatment group, indicating a reduction in the clearance of rMaspin during this time period (Fig. 6A). Protonation of chloroquine within the acidifying late endosome leads to an influx of H_2O and Cl^- with a resulting characteristic swelling of endosomal membranes. We observed a similar effect manifested as an increase in Rab9-positive endosome size in the chloroquine treatment group, confirming the activity of chloroquine on the endosomal pathway in our experiments (Fig. 6B). The number of these enlarged vesicles containing $rMaspin^{594}$ increased and corresponded to rMaspin levels observed by immunoblot analysis. $rMaspin^{594}$ continued to be trafficked to the lysosome under these conditions, demonstrating that chloroquine treatment did not block late endosome to lysosome fusion (Fig. 6C). Conversely, chloroquine treatment of endogenous Maspin-expressing MCF10A cells or MDA-MB-231 cells expressing the $Maspin^{EGFP}$ transgene had little effect on Maspin protein levels (Fig. 6D). These data indicate that genetically expressed Maspin is not turned over by the lysosomal pathway and endosomal sequestration is a consequence of exogenous application of Maspin protein.

Endosomal escape increases cytosolic rMaspin distribution and reduces lysosomal targeting

Finally, we evaluated the possibility that increases to rMaspin subcellular availability may be improved through mechanisms that promote endosomal escape of internalized proteins. To disrupt endosomes, we used Endo-porter, an

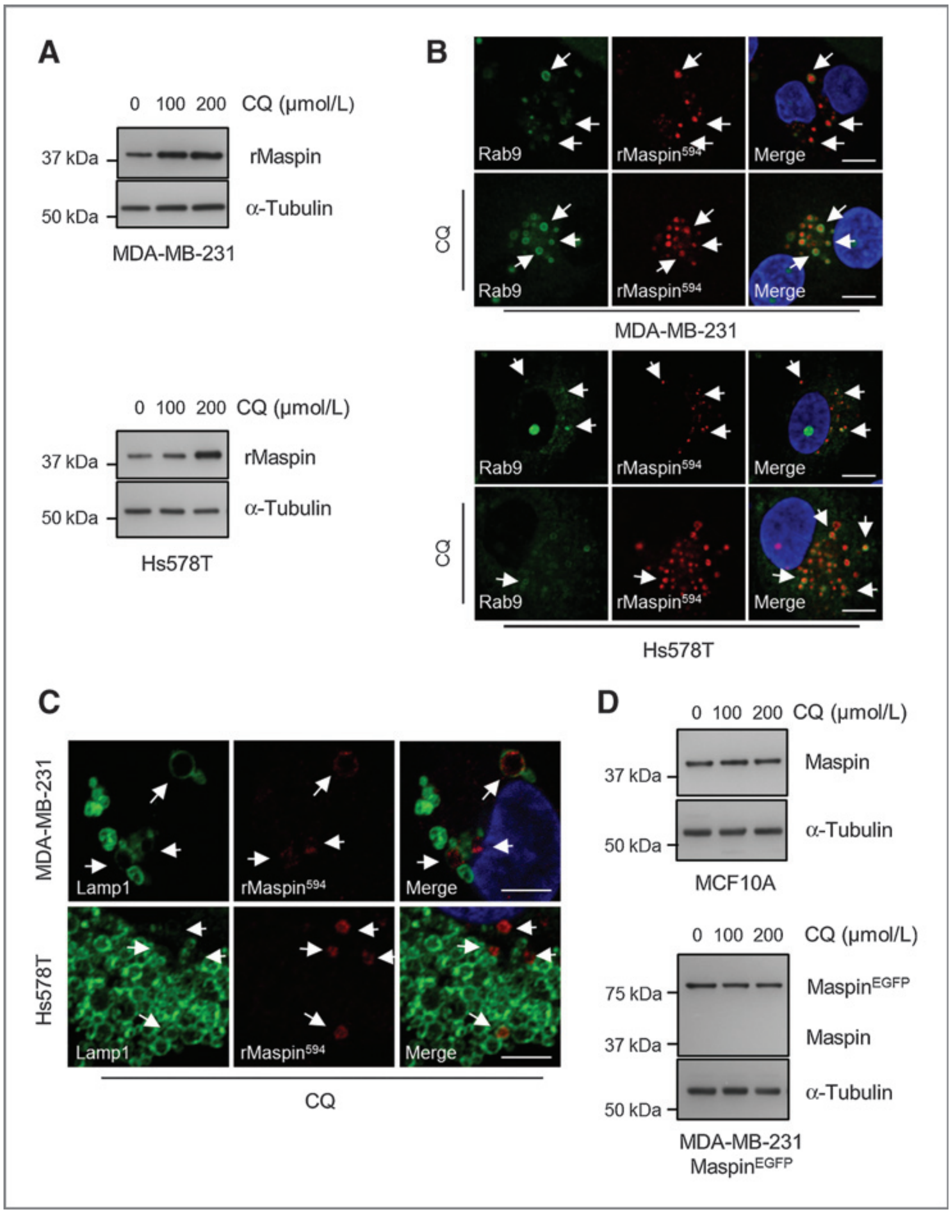

Figure 6. Lysosomal inhibition causes accumulation of rMaspin. A, MDA-MB-231 and Hs578T cells were treated with $rMaspin^{594}$ (10 μg/mL for 60 minutes) with or without chloroquine (CQ, 100–200 μmol/L; 30-minute pretreatment). Cell lysates were immunoblotted with Maspin and α-tubulin antibodies. B, MDA-MB-231 and Hs578T cells treated with $rMaspin^{594}$ (10 μg/mL for 60 minutes) with or without CQ (200 μmol/L; 30-minute pretreatment). $rMaspin^{594}$ fluorescence (red) was compared with Rab9 late endosomes (green) by confocal microscopy. C, MDA-MB-231 and Hs578T cells were treated as in B, and $rMaspin^{594}$ fluorescence (red) was compared with localization of Lamp1 lysosomes (green) by confocal microscopy. D, MCF10A endogenous Maspin-expressing cells and MDA-MB-231 cells transfected with a $Maspin^{EGFP}$ expression plasmid were treated with or without CQ (100–200 μmol/L for 90 minutes) and analyzed as in A. B and C, nuclei were counterstained with DAPI (blue); B, scale bar, 10 μm; C, scale bar, 5 μm.

amphiphilic peptide that induces endosomal rupture through pH changes following uptake by endocytosis. MDA-MB-231 cells were treated with rMaspin in the presence or absence of Endo-porter. Cells treated with Endo-porter exhibited a greater proportion of rMaspin^{594} distributed throughout the cytosol in a dose-dependent manner (Fig. 7A). Endo-porter induced a higher rate of rMaspin uptake; however, when rMaspin and Endo-porter were removed from culture media, internalized rMaspin was cleared at a slower rate in Endo-porter–treated cells (Fig. 7B). To better understand this, we analyzed endosomal trafficking under these conditions and revealed that rMaspin was no longer detected within late endosomes and targeting to lysosomes was reduced (Fig. 7C and D). These data collectively demonstrate a mechanism to reduce sequestering and clearance of rMaspin by the endosomal pathway, increasing half-life and allowing for the availability of rMaspin throughout the cell.

Discussion

Direct treatment of cancer cells with rMaspin produces inhibitory effects on cellular motility and demonstrates potential for therapeutic development. However, characterization of exogenously added rMaspin and uptake by cancer cells have not been described in detail. In this study, we have analyzed the processing of exogenously applied rMaspin into the endosomal pathway, with a resulting inhibition of invasion despite cytoplasmic sequestering. Specifically, we have characterized the uptake of rMaspin by multiple endocytic pathways and suggest a potential role for clathrin-mediated endocytosis on the inhibition of invasion.

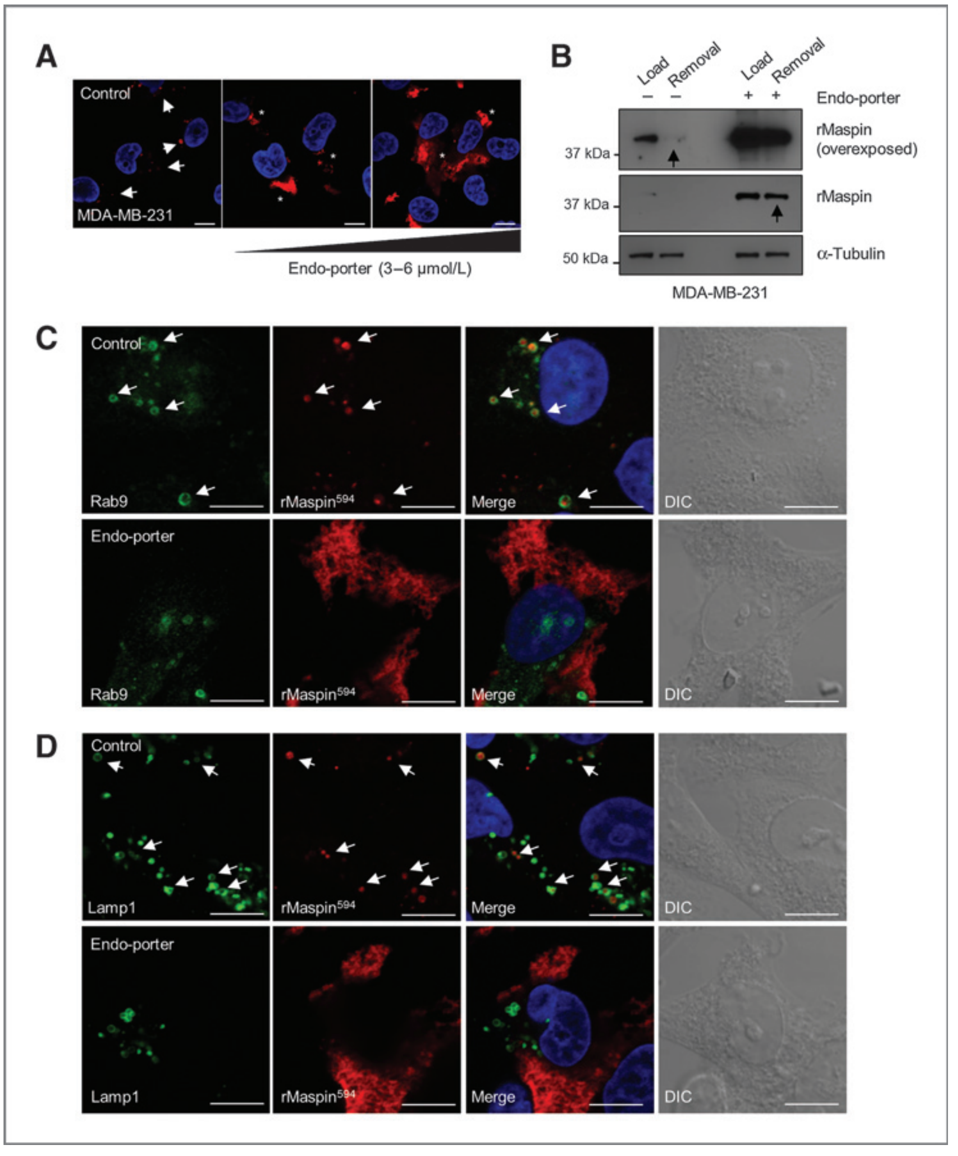

Figure 7. Endosomal escape leads to cytosolic distribution of rMaspin. A, MDA-MB-231 cells were treated with rMaspin^{594} (10 μg/mL for 120 minutes) in the presence or absence of increasing concentrations of Endo-porter (3–6 μmol/L) and rMaspin^{594} localization (red) analyzed by confocal microscopy. Arrows highlight vesicular rMaspin^{594}, asterisks highlight released rMaspin^{594}. B, MDA-MB-231 cells were treated with rMaspin (10 μg/mL for 60 minutes) with and without Endo-porter (6 μmol/L). Cells were then washed and grown in fresh media for an additional 60 minutes. Immunoblot analyses were probed with Maspin and α-tubulin antibodies. Arrows highlight levels of rMaspin that remained in cells 60 minutes after removal from media. C and D, MDA-MB-231 cells were treated with rMaspin^{594} (10 μg/mL for 120 minutes) with and without Endo-porter (6 μmol/L). Localization of rMaspin^{594} (red) was compared with Rab9 late endosomes (C, green) or Lamp1 lysosomes (D, green) by confocal microscopy. A, C, D, nuclei were counterstained with DAPI (blue); scale bar, 10 μm.

Endocytosis of receptors, attachment molecules, and other membrane components represents a means for regulating cellular motility, and this process is often dysregulated in cancer (18, 23, 26–34). The possibility that rMaspin may regulate signaling by endocytosis through interactions at the plasma membrane is strengthened by the established binding of Maspin with membrane components that alter extracellular matrix degradation, cell attachment, and migration (19, 20, 35–39). Although more work is needed to confirm this, our study is in line with a previous report by Biliran and Sheng which demonstrated that rMaspin was cleared from the cell surface of prostate cancer cells with simultaneous loss of uPA in an LRP1-dependent manner (40).

Following the early steps of endocytosis, we show the trafficking of rMaspin through the late stages of the endosomal pathway with localization in lysosomes. Treatment of cells with the endosomal/lysosomal inhibitor chloroquine increased rMaspin accumulation, indicating clearance by this mechanism. In addition, sequestering of rMaspin within this pathway reduces subcellular availability for potential cytosolic and nuclear functions. Endosomal escape of endocytosed proteins represents an approach to increase the efficacy of protein therapies (3, 41–46). We provide initial evidence that rMaspin can be released into the cytosol by permeation of endosomal membranes following internalization, leading to reduced clearance. However, cargo released from endosomes is subjected to low pH conditions and may affect structure and function. Future studies will be needed to address in detail the activity and regulation of rMaspin released by this approach. Additional findings indicate that nuclear localization of Maspin is important for its antitumor effects and correlates with better prognosis in patients with breast cancer (11, 47, 48). Although we did not observe nuclear translocation of rMaspin under our experimental conditions, interesting recent work has demonstrated a critical motif responsible for Maspin nuclear translocation that may potentially be modified to induce greater nuclear association of rMaspin in future experiments (49). Collectively, the characterization described in our study provides important information for the translational considerations about rMaspin.

Most recently, data have emerged that pose new questions related to the role of endogenously expressed Maspin in biology and disease (50). Although our study has focused on understanding the internalization and trafficking of exogenously applied rMaspin, we hope it will contribute new insights pertinent to the findings of previous reports. Our observations may also benefit future studies in which new utilities for Maspin are discovered, as the field acquires a more detailed understanding of Maspin function in human physiology.

Disclosure of Potential Conflicts of Interest

P.A. Pemberton has ownership interest (including patents) in SerPlus Technology LLC. No potential conflicts of interest were disclosed by the other authors.

Authors' Contributions

Conception and design: T.M. Bodenstine, R.E.B. Seftor, E.A. Seftor, P.A. Pemberton, M.J.C. Hendrix
Development of methodology: T.M. Bodenstine, R.E.B. Seftor, E.A. Seftor, Z. Khalkhali-Ellis
Acquisition of data (provided animals, acquired and managed patients, provided facilities, etc.): T.M. Bodenstine, R.E.B. Seftor, E.A. Seftor, N.A. Samii, J.C. Monarrez, G.S. Chandler
Analysis and interpretation of data (e.g., statistical analysis, biostatistics, computational analysis): T.M. Bodenstine, R.E.B. Seftor, M.J.C. Hendrix
Writing, review, and/or revision of the manuscript: T.M. Bodenstine, R.E.B. Seftor, E.A. Seftor, P.A. Pemberton, M.J.C. Hendrix
Administrative, technical, or material support (i.e., reporting or organizing data, constructing databases): P.A. Pemberton, M.J.C. Hendrix
Study supervision: M.J.C. Hendrix
Other (development and design of experiments, review and reading and correcting the manuscript): Z. Khalkhali-Ellis

Acknowledgments

The authors thank Bill Goossens for invaluable expertise on experiments utilizing instrumentation within the Stanley Manne Children's Research Institute Microscopy and Imaging Facility.

Grant Support

This work was supported by a grant from the NIH (to M.J.C. Hendrix; NIH CA75681). Additional support was received through a trainee award from the Northwestern University Robert H. Lurie Comprehensive Cancer Center's National Cancer Institute funded training program in Oncogenesis and Developmental Biology (T32 CA080621) and a Junior Investigator Award from the Brinson Foundation (to T.M. Bodenstine).

The costs of publication of this article were defrayed in part by the payment of page charges. This article must therefore be hereby marked *advertisement* in accordance with 18 U.S.C. Section 1734 solely to indicate this fact.

Received January 31, 2014; revised May 28, 2014; accepted June 23, 2014; published OnlineFirst September 25, 2014.

References

1. Siegel R, Ma J, Zou Z, Jemal A. Cancer statistics, 2014. CA Cancer J Clin 2014;64:9–29.
2. Leader B, Baca QJ, Golan DE. Protein therapeutics: a summary and pharmacological classification. Nat Rev Drug Discov 2008; 7:21–39.
3. Pisal DS, Kosloski MP, Balu-Iyer SV. Delivery of therapeutic proteins. J Pharm Sci 2010;99:2557–75.
4. Zou Z, Anisowicz A, Hendrix MJ, Thor A, Neveu M, Sheng S, et al. Maspin, a serpin with tumor-suppressing activity in human mammary epithelial cells. Science 1994;263:526–9.
5. Denk AE, Bettstetter M, Wild PJ, Hoek K, Bataille F, Dietmaier W, et al. Loss of maspin expression contributes to a more invasive potential in malignant melanoma. Pigment Cell Res 2007;20: 112–9.
6. Bailey CM, Khalkhali-Ellis Z, Seftor EA, Hendrix MJ. Biological functions of maspin. J Cell Physiol 2006;209:617–24.
7. Seftor RE, Seftor EA, Sheng S, Pemberton PA, Sager R, Hendrix MJ. maspin suppresses the invasive phenotype of human breast carcinoma. Cancer Res 1998;58:5681–5.
8. Khalkhali-Ellis Z, Hendrix MJ. Elucidating the function of secreted maspin: inhibiting cathepsin D-mediated matrix degradation. Cancer Res 2007;67:3535–9.
9. Goulet B, Chan G, Chambers AF, Lewis JD. An emerging role for the nuclear localization of maspin in the suppression of tumor progression and metastasis. Biochem Cell Biol 2012;90:22–38.
10. Narayan M, Twining S. Focus on molecules: maspin. Exp Eye Res 2010;90:2–3.
11. Berardi R, Morgese F, Onofri A, Mazzanti P, Pistelli M, Ballatore Z, et al. Role of maspin in cancer. Clin Transl Med 2013;2:8.
12. Sheng S, Pemberton PA, Sager R. Production, purification, and characterization of recombinant maspin proteins. J Biol Chem 1994;269: 30988–93.

13. Sheng S, Carey J, Seftor EA, Dias L, Hendrix MJ, Sager R. Maspin acts at the cell membrane to inhibit invasion and motility of mammary and prostatic cancer cells. Proc Natl Acad Sci U S A 1996;93:11669–74.

14. Jiang N, Meng Y, Zhang S, Mensah-Osman E, Sheng S. Maspin sensitizes breast carcinoma cells to induced apoptosis. Oncogene 2002;21:4089–98.

15. Li Z, Shi HY, Zhang M. Targeted expression of maspin in tumor vasculatures induces endothelial cell apoptosis. Oncogene 2005;24: 2008–19.

16. Hendrix MJ, Seftor EA, Seftor RE, Fidler IJ. A simple quantitative assay for studying the invasive potential of high and low human metastatic variants. Cancer Lett 1987;38:137–47.

17. Seftor EA, Meltzer PS, Kirschmann DA, Pe'er J, Maniotis AJ, Trent JM, et al. Molecular determinants of human uveal melanoma invasion and metastasis. Clin Exp Metastasis 2002;19:233–46.

18. McMahon HT, Boucrot E. Molecular mechanism and physiological functions of clathrin- mediated endocytosis. Nat Rev Mol Cell Biol 2011;12:517–33.

19. Al-Ayyoubi M, Schwartz BS, Gettins PG. Maspin binds to urokinase-type and tissue-type plasminogen activator through exosite–exosite interactions. J Biol Chem 2007;282:19502–9.

20. Cella N, Contreras A, Latha K, Rosen JM, Zhang M. Maspin is physically associated with [beta]1 integrin regulating cell adhesion in mammary epithelial cells. FASEB J 2006;20:1510–2.

21. Doherty GJ, McMahon HT. Mechanisms of endocytosis. Annu Rev Biochem 2009;78:857–902.

22. Lillis AP, Van Duyn LB, Murphy-Ullrich JE, Strickland DK. LDL receptor-related protein 1: unique tissue-specific functions revealed by selective gene knockout studies. Physiol Rev 2008; 88:887–918.

23. Mayor S, Pagano RE. Pathways of clathrin-independent endocytosis. Nat Rev Mol Cell Biol 2007;8:603–12.

24. Ivanov AI. Pharmacological inhibition of endocytic pathways: is it specific enough to be useful? Methods Mol Biol 2008;440:15–33.

25. de Duve C, de Barsy T, Poole B, Trouet A, Tulkens P, Van Hoof F. Commentary. Lysosomotropic agents. Biochem Pharmacol 1974;23: 2495–531.

26. Di Guglielmo GM, Le Roy C, Goodfellow AF, Wrana JL. Distinct endocytic pathways regulate TGF-beta receptor signalling and turnover. Nat Cell Biol 2003;5:410–21.

27. Lim JP, Gleeson PA. Macropinocytosis: an endocytic pathway for internalising large gulps. Immunol Cell Biol 2011;89:836–43.

28. Gu Z, Noss EH, Hsu VW, Brenner MB. Integrins traffic rapidly via circular dorsal ruffles and macropinocytosis during stimulated cell migration. J Cell Biol 2011;193:61–70.

29. Upla P, Marjomaki V, Kankaanpaa P, Ivaska J, Hyypia T, Van Der Goot FG, et al. Clustering induces a lateral redistribution of alpha 2 beta 1 integrin from membrane rafts to caveolae and subsequent protein kinase C-dependent internalization. Mol Biol Cell 2004;15: 625–36.

30. Ezratty EJ, Bertaux C, Marcantonio EE, Gundersen GG. Clathrin mediates integrin endocytosis for focal adhesion disassembly in migrating cells. J Cell Biol 2009;187:733–47.

31. Mellman I, Yarden Y. Endocytosis and cancer. Cold Spring Harb Perspect Biol 2013;5:a016949.

32. Mosesson Y, Mills GB, Yarden Y. Derailed endocytosis: an emerging feature of cancer. Nat Rev Cancer 2008;8:835–50.

33. Goldenring JR. A central role for vesicle trafficking in epithelial neoplasia: intracellular highways to carcinogenesis. Nat Rev Cancer 2013;13:813–20.

34. McGowen R, Biliran H Jr, Sager R, Sheng S. The surface of prostate carcinoma DU145 cells mediates the inhibition of urokinase-type plasminogen activator by maspin. Cancer Res 2000;60:4771–8.

35. Yin S, Lockett J, Meng Y, Biliran H Jr, Blouse GE, Li X, et al. Maspin retards cell detachment via a novel interaction with the urokinase-type plasminogen activator/urokinase- type plasminogen activator receptor system. Cancer Res 2006;66:4173–81.

36. Seftor REB, Odero VA, Seftor EA, Hendrix MJC. *Maspin* suppresses breast cancer invasiveness by modulating integrin expression and function. Georgetown: Landes Bioscience 2002;*Maspin*:84–95.

37. Qin L, Zhang M. Maspin regulates endothelial cell adhesion and migration through an integrin signaling pathway. J Biol Chem 2010; 285:32360–9.

38. Bass R, Wagstaff L, Ravenhill L, Ellis V. Binding of extracellular maspin to beta1 integrins inhibits vascular smooth muscle cell migration. J Biol Chem 2009;284:27712–20.

39. Endsley MP, Hu Y, Deng Y, He X, Warejcka DJ, Twining SS, et al. Maspin, the molecular bridge between the plasminogen activator system and beta1 integrin that facilitates cell adhesion. J Biol Chem 2011;286:24599–607.

40. Biliran H Jr, Sheng S. Pleiotrophic inhibition of pericellular urokinase-type plasminogen activator system by endogenous tumor suppressive maspin. Cancer Res 2001;61:8676–82.

41. Cronican JJ, Thompson DB, Beier KT, McNaughton BR, Cepko CL, Liu DR. Potent delivery of functional proteins into Mammalian cells *in vitro* and *in vivo* using a supercharged protein. ACS Chem Biol 2010;5: 747–52.

42. Madani F, Lindberg S, Langel U, Futaki S, Graslund A. Mechanisms of cellular uptake of cell-penetrating peptides. J Biophys 2011;2011: 414729.

43. Swaminathan J, Ehrhardt C. Liposomal delivery of proteins and peptides. Expert Opin Drug Deliv 2012;9:1489–503.

44. Varkouhi AK, Scholte M, Storm G, Haisma HJ. Endosomal escape pathways for delivery of biologicals. J Control Release 2011;151: 220–8.

45. Nakase I, Kobayashi S, Futaki S. Endosome-disruptive peptides for improving cytosolic delivery of bioactive macromolecules. Biopolymers 2010;94:763–70.

46. Erazo-Oliveras A, Muthukrishnan N, Baker R, Wang TY, Pellois JP. Improving the endosomal escape of cell-penetrating peptides and their cargos: strategies and challenges. Pharmaceuticals 2012;5: 1177–209.

47. Li X, Yin S, Meng Y, Sakr W, Sheng S. Endogenous inhibition of histone deacetylase 1 by tumor-suppressive maspin. Cancer Res 2006;66: 9323–9.

48. Goulet B, Kennette W, Ablack A, Postenka CO, Hague MN, Mymryk JS, et al. Nuclear localization of maspin is essential for its inhibition of tumor growth and metastasis. Lab Invest 2011;91:1181–7.

49. Dzinic SH, Kaplun A, Li X, Bernardo M, Meng Y, Dean I, et al. Identification of an intrinsic determinant critical for maspin subcellular localization and function. PLoS ONE 2013;8:e74502.

50. Teoh SS, Vieusseux J, Prakash M, Berkowicz S, Luu J, Bird CH, et al. Maspin is not required for embryonic development or tumour suppression. Nat Commun 2014;5:3164.